ORNL/TM-2017/153

Nuclear Hybrid Energy System Model Stability Testing

M. S. Greenwood
M. S. Cetiner
D. L. Fugate

March 2017

**Approved for public release.
Distribution is unlimited.**

OAK RIDGE NATIONAL LABORATORY
MANAGED BY UT-BATTELLE FOR THE US DEPARTMENT OF ENERGY

ORNL/TM-2017/153

Reactor and Nuclear Systems Division
Electrical and Electronics Systems Research Division

NUCLEAR HYBRID ENERGY SYSTEM MODEL STABILITY TESTING

M. S. Greenwood
M. S. Cetiner
D. L. Fugate

Date Published: March 2017

Prepared by
OAK RIDGE NATIONAL LABORATORY
Oak Ridge, TN 37831-6283
managed by
UT-BATTELLE, LLC
for the
US DEPARTMENT OF ENERGY
under contract DE-AC05-00OR22725

CONTENTS

LIST OF FIGURES

LIST OF TABLES

ACRONYMS AND ABBREVIATIONS

AIC	Akaike information criterion
ANL	Argonne National Laboratory
BOP	balance of plant
CPU	central processing unit
EG	electrical grid
EIA	US Energy Information Administration
EM	energy manifold
EPRI	Electric Power Research Institute
ES	energy storage
FOM	figure of merit
HPC	high-performance cluster
INL	Idaho National Laboratory
IC	information criterion
IP	industrial process
IRIS	International Reactor Innovative and Secure
MB	megabyte
MHz	megahertz
MJ	megajoules
MPa	megapascal
MWehr	megawatt-hours electric
NHES	Nuclear Hybrid Energy System
ORNL	Oak Ridge National Laboratory
PHS	primary heat system
PI	proportional-integral
Probit	Probability Unit
RNSD	Reactor and Nuclear Systems Division
SC	supervisory control
SES	secondary energy supply
SY	switchyard
VM	virtual machine

ABSTRACT

A Nuclear Hybrid Energy System (NHES) uses a nuclear reactor as the basic power generation unit, and the power generated is used by multiple customers as combinations of thermal power or electrical power. The definition and architecture of a particular NHES can be adapted based on the needs and opportunities of different localities and markets. For example, locations in need of potable water may be best served by coupling a desalination plant to the NHES. Similarly, a location near oil refineries may have a need for emission-free hydrogen production. Using the flexible, multi-domain capabilities of Modelica, Argonne National Laboratory, Idaho National Laboratory, and Oak Ridge National Laboratory are investigating the dynamics (e.g., thermal hydraulics and electrical generation/consumption) and cost of a hybrid system. This paper examines the NHES work underway, emphasizing the control system developed for individual subsystems and the overall supervisory control system.

1. INTRODUCTION

Electricity markets in the United States are undergoing significant shifts in the traditional market structure. Factors such as mandates for renewable energy, overall carbon reduction, and the emergence of low cost natural gas supplies have strained the profitability of traditional baseload electricity suppliers, including nuclear power plants.

As the typical nuclear power generating station traditionally has only one customer—the grid—diversification of the customer portfolio in an integrated or hybrid manner may be advantageous. A representative NHES is depicted in Figure 1.

A hybrid energy system approach that couples base load energy suppliers and various energy customers (thermal and/or electric) may be profitable and preferred in future energy markets. Possible scenarios include product options that could be more profitable than traditional electricity generation. This could mitigate the possible load-following need—and subsequent cost increases—that significant renewable penetration may impose on nuclear power plants. For example, Figure 2 is a representative summary of the recent study conducted by the Electric Power Research Institute (EPRI) to determine the impact of renewable energy generation on grid variability (EPRI 2015). Given current economic and political trends, future electrical grids will require highly variable operations that impose significant technical and economic challenges for power producers. Introducing hybrid energy systems may help create a path to achieving highly variable markets that are economically sound and do not compromise grid reliability.

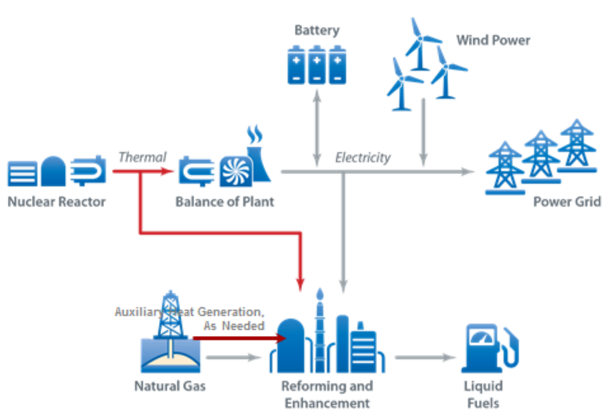

Figure 1. A representative NHES demonstrating a possible coupling scenario of both thermal and electrical energy with additional systems (e.g., an industrial process and energy storage system) (Bragg-Sitton 2015)**.**

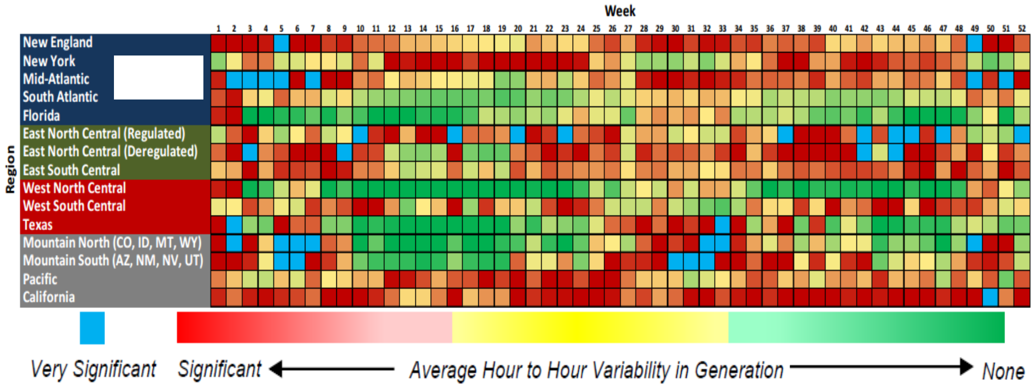

Figure 2. Prediction of electrical grid variability for US regions in 2050. The color of the cells represents the variability. Regions approaching red and blue have demands that will be difficult and expensive for the electrical grid to meet—especially power producers operating under traditional market paradigms (EPRI 2015)**.**

Three national laboratories are working on defining, designing, analyzing, and optimizing nuclear hybrid systems. Idaho National Laboratory (INL) is the lead lab working with Argonne National Laboratory (ANL) and Oak Ridge National Laboratory (ORNL). Each laboratory provides modeling and simulation expertise to integrate the hybrid system.

1.1 DEFINITION OF NUCLEAR HYBRID SYSTEMS

A nuclear hybrid system uses a nuclear reactor as the basic power generation unit. The power generated by the nuclear reactor is used by one or more power customers as thermal power, electrical power, or both. A nuclear hybrid system couples the nuclear reactor to at least one thermal power user, in addition to the power conversion system.

The definition and architecture of a particular nuclear hybrid system vary depending on local market needs and opportunities. For example, locations in need of potable water may be served best by a desalination plant coupled to the nuclear system. Similarly, an area near oil refineries may have a need for near-zero-emission hydrogen production. A nuclear hybrid system expands the nuclear power plant from its more familiar central power station role by diversifying its customer base through immediate, direct connection.

1.2 CONTEXT OF NUCLEAR HYBRID SYSTEMS

A nuclear hybrid system can provide options to avoid the sale of electricity in unfavorable electricity market conditions. This is especially important for deregulated wholesale electricity markets with long price distribution tails. For example, the price rarely approaches \$0/MWehr (EIA 2016a), and the average for the wholesale price in some markets is around \$27/MWehr (EIA 2016a), but the high end can reach more than \$100/MWehr (EIA 2016b). On the low end of the distribution, the market prices may fall negative in some situations, forcing the nuclear reactor operators to decide whether to endure economic loss conditions or to curtail power generation. Neither approach is attractive. A potential benefit is to help accommodate an increased share of renewable power on the grid. As renewable generation increases, the volatility of the grid increases in response to the intermittent nature of the renewable generation. Typically, the grid volatility is smoothed by using natural gas generators as backups to the renewable sources because of their rapid response characteristics. However, the use of gas generators reintroduces carbon emissions that renewable sources originally displaced. Even if technically capable, nuclear reactor operators may not want to use their reactors in a load-following mode due to concerns about thermal and chemical cycling. However, with the addition of a flexible resource in the form of a nuclear hybrid system, overall grid volatility can be tempered.

1.3 PERFORMANCE GOALS OF NUCLEAR HYBRID SYSTEMS

A goal of the Nuclear Hybrid Energy System (NHES) project is to compare the enhanced performance of integrated systems to independent stand-alone systems. The most illustrative, direct comparison of the performance is captured through cost analyses. The construction, operations, and fuel costs for the reactor, power conversion, and other coupled systems are typically well documented, or they can be estimated based on historical data or other information such as the Advanced Fuel Cycle Cost Basis (Shropshire 2007). External costs such as carbon emissions can be accounted for based on estimated or assumed values. Comparisons of other important figures of merit (FOMs), such as system reliability/availability and induced grid stability, require additional estimation.

1.4 PURPOSE OF THIS REPORT

This report documents work performed at ORNL to produce dynamic models to analyze NHESs. This work describes the current implementation of each component or subsystem model as well as the integration of component or subsystem models developed by INL or ANL. It also describes the overall system that defines the initial base case for NHES analysis. Finally, it presents the results from a parametric sweep of several simulation and model parameters.

2. NHES DYNAMIC MODEL

2.1 MODELICA

Modelica (Mod. Assoc. 2017) is a nonproprietary, object-oriented, equation-based programming language used to conveniently model complex physical and cyber-physical systems (e.g., systems containing mechanical, electrical, electronic, hydraulic, thermal, and control components). Given the complex, diverse range of physics involved in modeling a dynamic hybrid energy system, the multi-domain nature of Modelica was selected for its flexibility in modeling the appropriate physics of all systems and associated control systems using one tool.

An example of Modelica’s modeling method can be characterized by Figure 3, which demonstrates creation of generic models linked to create ever more complex models. Verification tests can be performed to investigate the behavior of the model.

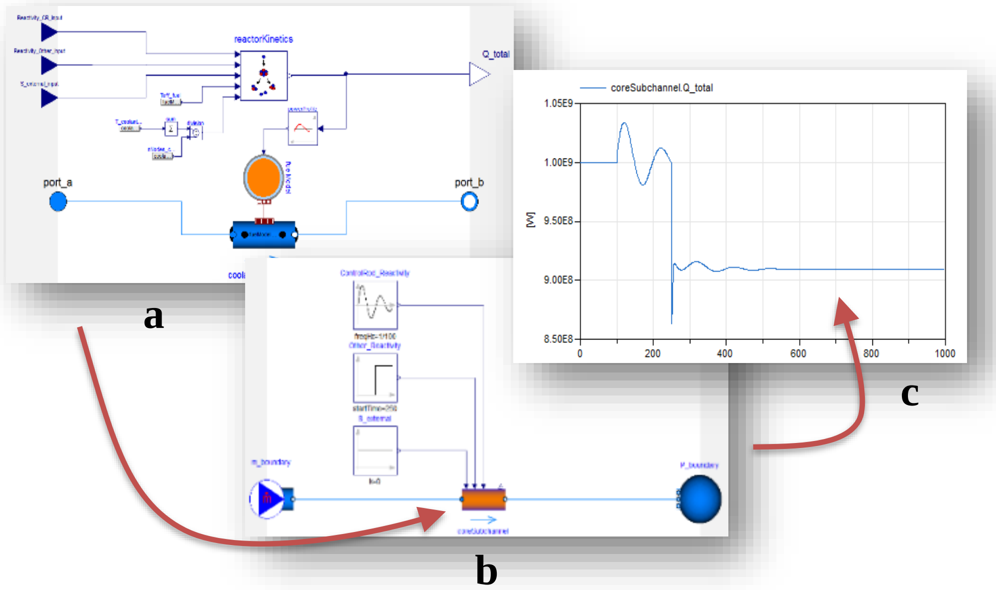

Figure 3. (a) Creation of a more complex model from several individual models describing different physics based systems, (b) reactor core sub channel model created and tested, and (c) behavior of the generated system in the assembled test case (e.g., total thermal output).

2.2 THE TIGHTLY COUPLED NHES

The reference hybrid energy system is referred to as a "*tightly coupled*" system. This coupling indicates that both the thermal and the electrical energy from the base load power supplier are integrated with one or more systems (e.g., industrial plant). The Modelica-based system under development is presented in Figure 4. The numbers in the figure correspond to the brief descriptions in Table 1. The dynamic model is used to provide non-economic figures of merit such as the ability to meet specified energy demands and overall system stability and reliability to supplement the economic cost evaluation.

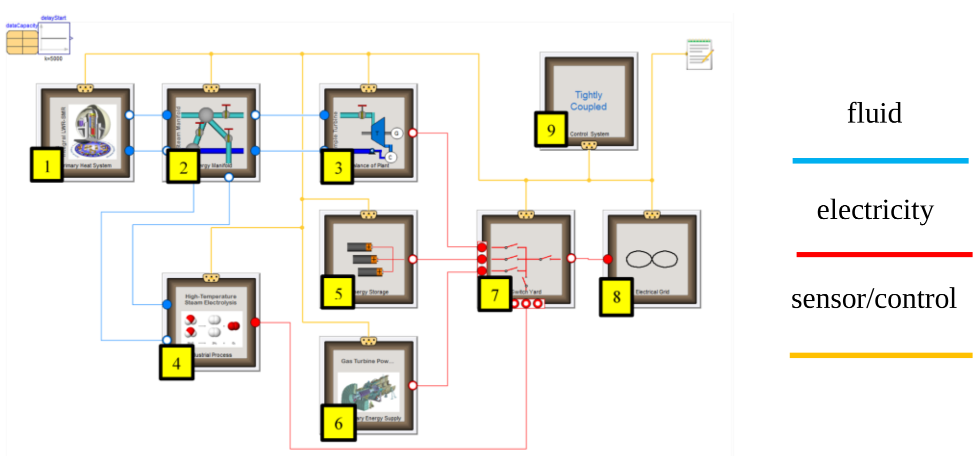

Figure 4. Tightly coupled NHES under development.

Table 1. Description of subsystems comprising a tightly coupled hybrid energy system

Identifier	Component	Description	Example
1	Primary Heat System (PHS)	Provides baseload heat and power	Nuclear reactor
2	Energy Manifold (EM)	Diverts thermal energy between subsystems	Steam distribution
3	Balance of Plant (BOP)	Serves as primary electricity supply from energy not used in other subsystems.	Turbine and condenser
4	Industrial Process (IP)	Generates high value product using heat from the energy manifold/secondary energy supply and electricity from the switchyard.	Steam electrolysis or desalination
5	Energy Storage (ES)	Serves as energy buffer to increase overall system robustness.	Batteries and firebrick
6	Secondary Energy Supply (SES)	Delivers small amounts of topping heat required by industrial process.	Gas turbine make-up
7	Switchyard (SY)	Distributes electrical load between subsystems.	Electricity distribution
8	Electrical Grid (EG)	Sets the behavior of the grid connected to the NHES	Large grid behavior (not influenced by NHES)
9	Control System Center	Additional systems required to provide proper system control, test scenarios, etc.	Control/supervisory systems and event drivers

2.2.1 Primary Heat System (PHS)

The current NHES under investigation employs an integral pressurized water nuclear reactor based on the International Reactor Innovative and Secure (IRIS) (Westinghouse 2007). A few important physical phenomena captured in the model include the two-phase dynamic interactions of the pressurizer, the generation of steam in a helical coil steam generator, and the behavior of the nuclear core. The nuclear core model is shown in Figure 5, and its associated control system is depicted in Figure 6. This model integrates the coolant flow geometry and behavior, fuel behavior, and point kinetics neutronics behavior, with feedback from the fuel and coolant temperatures. Current implementation of the core dynamics does not account for burnup or the impact of isotopic fuel changes.

The control system monitors the total core power and controls the core rod reactivity to hold the PHS thermal power at the nominal state of 1,000 MW. The controller is a standard proportional-integral (PI) controller with inputs normalized to approximately 1 to assist the solver with the numerical solution. Currently the system pressure is permitted to fluctuate within approximately 0.5 MPa of the nominal condition of 15.5 MPa. The liquid heaters of the pressurizer use a simple on/off controller with hysteresis that adds heat to increase system pressure when the monitored pressure drops to 15.0 MPa. This fluctuation range and control method may be revisited to investigate better, alternative methods.

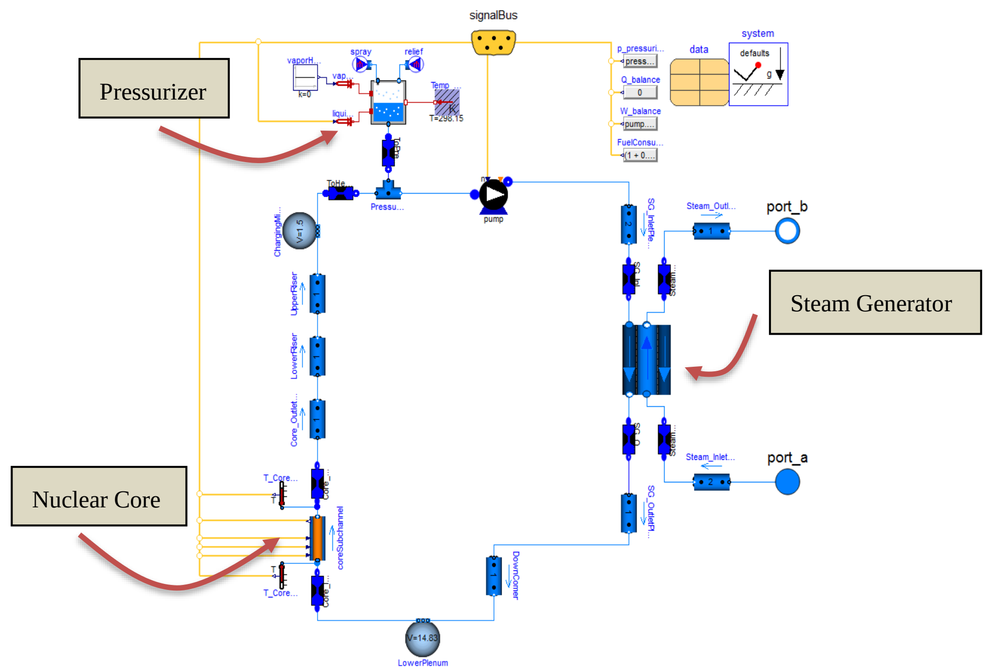

Figure 5. Modelica model of the PHS based on the IRIS reactor. The current implementation of this system requires only two controllers to keep the operation of the reactor stable, control rod reactivity control based on total power and pressure control with heaters in the pressurizer.

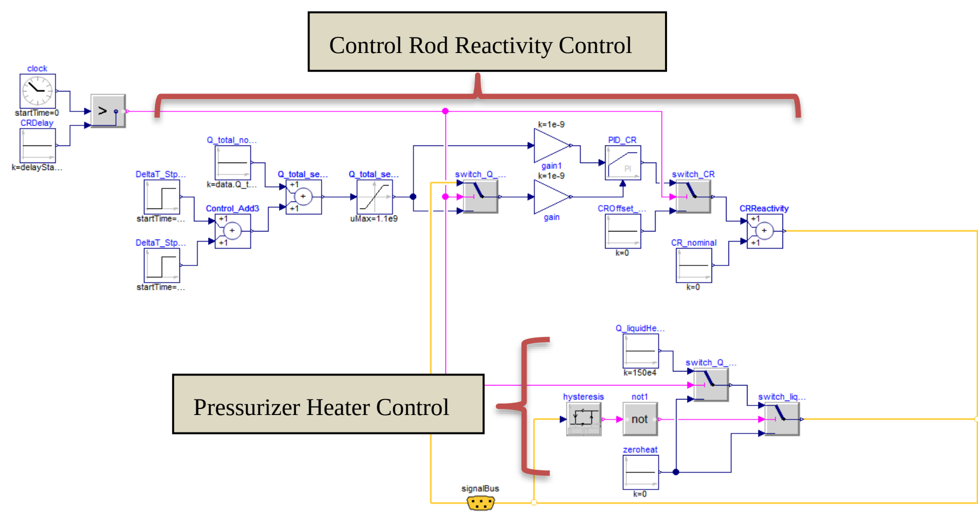

Figure 6. Control system for the IRIS PHS based on total core power and system pressure.

2.2.2 Energy Manifold (EM)

The current EM under consideration is a purely thermal (i.e., steam/water) manifold (Figure 7). The EM relies on controller logic to actuate distribution valves to handle large and slow power set point changes to other subsystems, as specified by the demand profile. This actuation diverts hot steam coming from the PHS to the desired destination. The manifold also gathers return streams and directs the flow back to the PHS steam generator at the proper temperature and pressure. Mixing and splitting volumes then add thermal mass to the system, dampening transient behaviors.

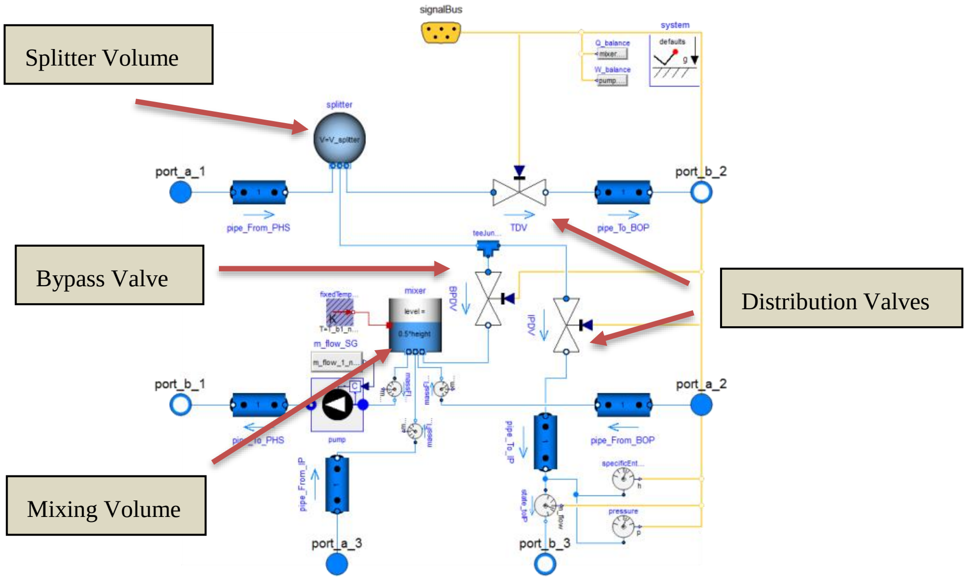

Figure 7. EM for distributing and gathering steam/water streams from sub systems. The bypass valve is important for dampening pressure responses of the system when tracking demand profiles. The splitter and mixing volumes dampen transient thermal behavior.

The EM control system (Figure 8) monitors the demand power set points of the BOP and actuates the turbine distribution valve to track the power using a PI controller. The bypass valve acts in a directly opposite response to the turbine distribution valve to limit system pressure swings. The position of the valve to the industrial process is held at a nominal point to set by the nominal operating point of the process. The industrial process then controls the flow rate it receives based on its internal pressure drop.

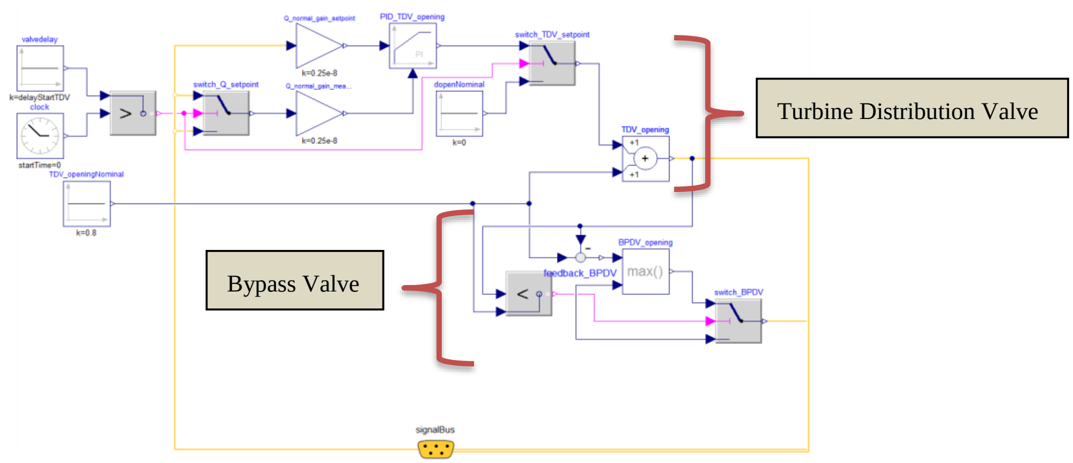

Figure 8. EM control system. The turbine distribution valve is actuated to meet the demand profile set points of the BOP while the bypass valve acts exactly opposite of the turbine distribution valve to dampen pressure swings within the system.

2.2.3 Balance of Plant (BOP)

The BOP receives steam from the EM and generates electrical power to send to the SY (Figure 9). The steam passes through a control valve to a steam turbine modeled using Stodola's law of infinite stages. The outflow of the turbine passes to an ideal condenser and then gets pumped back to the EM. The current basic implementation of the BOP requires no active control system. The power from the generator is monitored by the EM control system which then actuates the turbine distribution valve in the EM as appropriate.

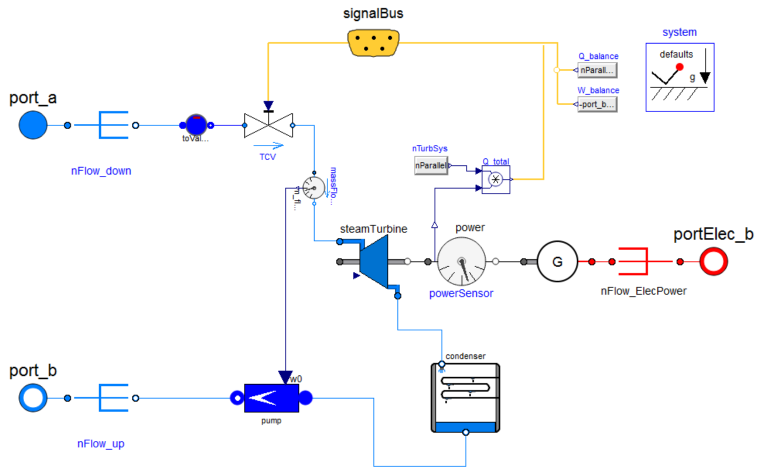

Figure 9. BOP model which produces the primary source of NHES electrical energy.

2.2.4 Energy Storage (ES)

The ES system is a logic-based controller (no explicit physics) of a battery system (Figure 10) modeled in collaboration with ANL. The model contains a capacitive term that represents the charge level of the battery. The logic keeps the battery within a specified minimum and maximum capacity and allows the charge and discharge rates to be limited independently. The set point of the battery is provided by the supervisory control system and the logic integrates the behavior with an electrical power port that ties into the SY. Although it is technically non-physical, this model contains appropriate logic that mirrors the physical behavior of a generic ES system at a high level. No additional control system is required for this model.

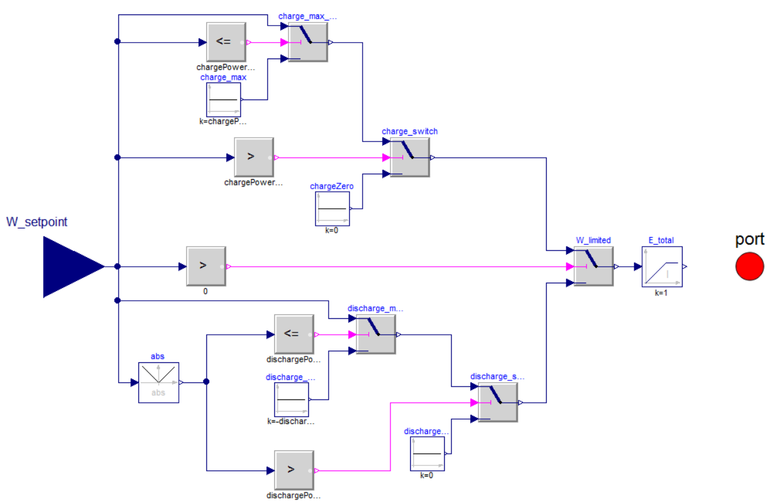

Figure 10. Logic-based implementation of a basic energy storage subsystem that takes a power set point and strives to meet that set point within the limitations of the user-specified parameters (capacity, charge rates, etc.).

2.2.5 Secondary Energy Supply (SES)

The SES is a natural gas-fired turbine power plant modeled by INL (Figure 11). The controls for this model are imbedded within the physical model and therefore do not have a separate control system. Like the ES system, this model takes a power demand signal from the supervisory control system and seeks to match it within the physical limitations of the model.

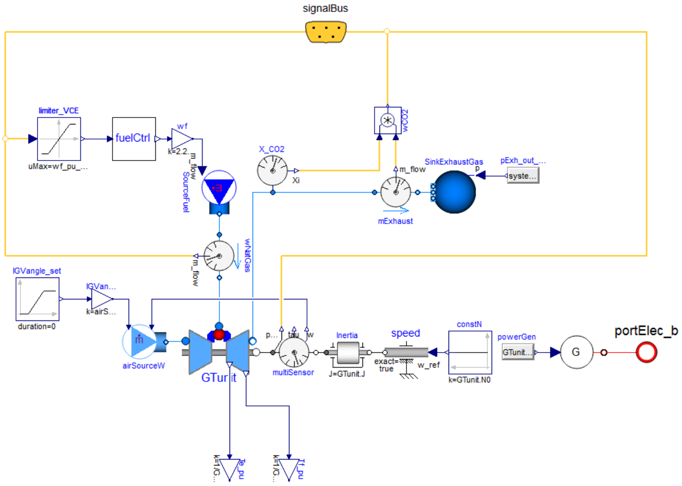

Figure 11. Model of a natural gas-fired power plant for use as an SES provided by INL. The power output is defined by the supervisory control system.

2.2.6 Industrial Process (IP)

The IP being used in the current study is a high–temperature steam electrolysis plant for hydrogen production modeled by INL (Figure 12). The controls for this model are imbedded within the physical model and therefore do not have a separate control system. The model consumes electricity from the SY proportional to the amount of steam received from the EM.

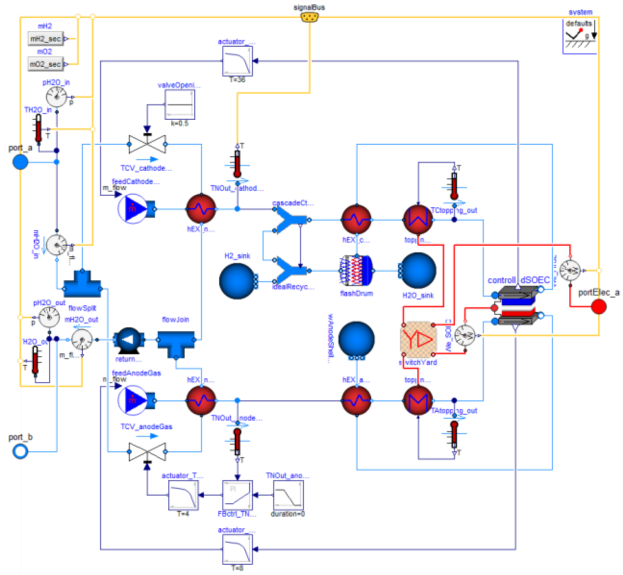

Figure 12. Model of high-temperature steam electrolysis plant for hydrogen gas production provided by INL.

2.2.7 Switchyard (SY) and Electrical Grid (EG)

The SY provides a common distribution block for electrical power to the various subsystems of the NHES and the EG (Figure 13). The EG is an infinite sink/source of electrical power that set the frequency of the electricity to 60 Hz. There are no explicit controls for the current basic SY or EG—only measurement devices that log the power produced/consumed by a given subsystem.

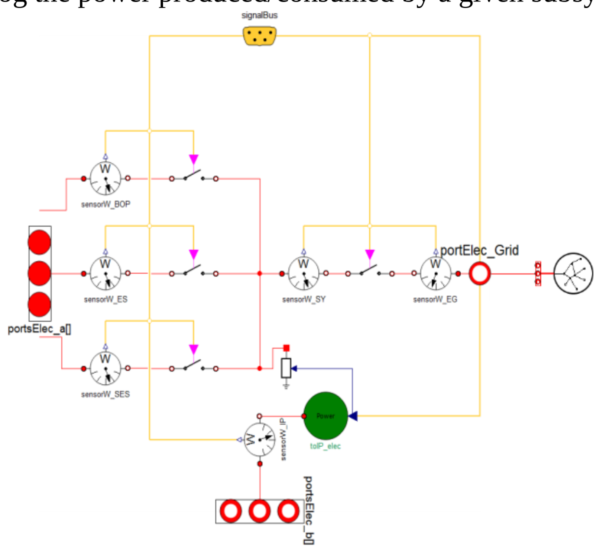

Figure 13. Basic SY which gathers and provides a common line for power distribution between all subsystems and the EG. The EG is modeled as an infinite sink/source that sets the frequency of the electrical power.

2.2.8 Supervisory Control (SC) System

The SC system is responsible for providing the over-arching guidance of NHES behavior. In the RAVEN optimization framework, power demand profiles are generated for the BOP, ES, and SES (Figure 14). These set points are then imposed on the appropriate system by subsystem controls. The EG demand can also be read into the simulation but is currently only used for reference and not for any explicit control operation.

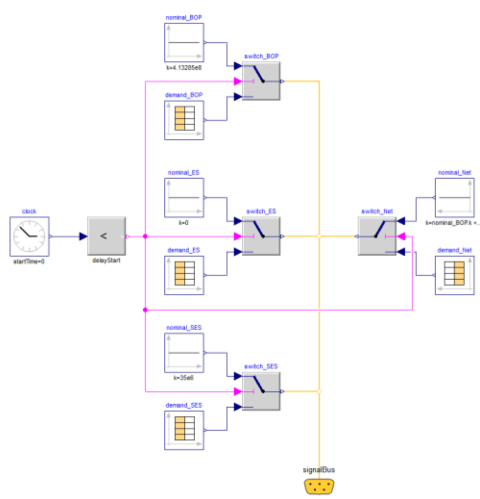

Figure 14. The SC system reads power demand set points for the BOP, ES, and SES from an external file. These signals set the behavior of the system via the lower level control logic of individual subsystems. The EG set point is also read but is provided only for reference.

2.3 HYBRID SYSTEMS DYNAMICS

The initial development of the dynamic system imposed fixed nominal parameters (Table 2) to focus on creating a functional, integrated system. The following figures demonstrate the dynamic behavior of this simulation by having the BOP, ES, and SES follow electricity demand power set points from the SC system. The simulation consisted of 14581 equations and simulated a one-week period in 2.3 hours using Dymola 2017 FD01 on a desktop computer (16 GB ram, Intel Xeon CPU ES-1607 v3 @ 3.10GHz).

Table 2. Fixed nominal parameters for initial system development

Type	Parameter	Value
Simulation Parameter	Tolerance	1e-8
	Increments/Intervals	1 interval every 10 sec
	Simulation time	1 Week
Model Parameter	ES Capacity	20 MWehr
	Pipe length to BOP from EM	1 m
	Pipe length to IP from EM	1 m
	EM Splitter volume	10 m^3
	EM Mixer volume	10 m^3

Figure 15 depicts the behavior of the pressurizer pressure in the PHS. The pressure slowly decreases over time due to ingress of cooler primary loop water into the pressurizer. Eventually the pressurizer liquid cools enough that the liquid heater control turns on until the pressure rises back to the nominal 15.5 MPa. This is a cyclic behavior that continues throughout the simulation; frequency depends on the dynamics of the EM.

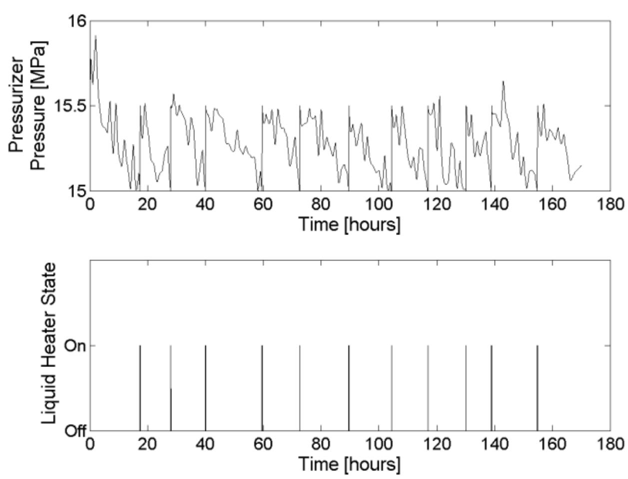

Figure 15. Pressurizer pressure in the PHS depicting an oscillatory behavior due to dynamics of the EM and the liquid heater compensation to raise the pressure from the minimum 15.0 MPa to the nominal 15.5 MPa.

Figure 16 demonstrates the ability of the system to be held relatively constant at the nominal thermal operating power of 1000 MW using only control rod reactivity control. The behavior shown depends on the behavior of the EM via the dynamic boundary conditions of the steam side of the helical coil steam generator.

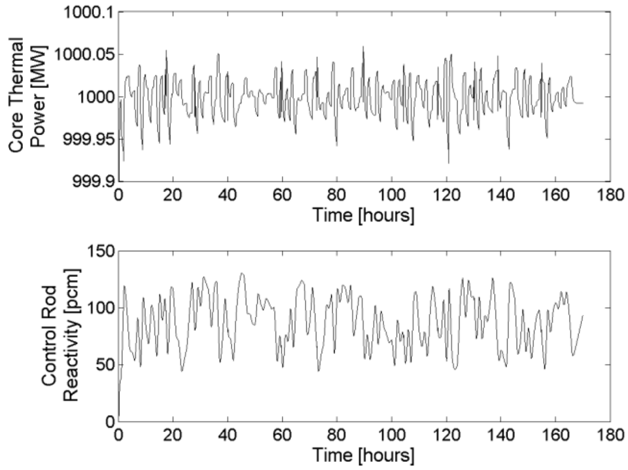

Figure 16. Core thermal power and control rod reactivity behavior necessary to keep the PHS operating at a nominal thermal power level of 1000 MW.

Figure 17 demonstrates the actuation of the valves in the EM that are required to match the aggressive demand profile. The valves act opposite of each other to limit the impacts on other subsystems (e.g., significant pressure deviations from nominal). Physical limitations of the system (e.g., transport delay, pressure limits) prevent exact following of the set point. However, in addition to physical limitations, the PI controller parameters also can have a significant impact on the ability of the system to precisely load follow. This may be an area of additional research in the future.

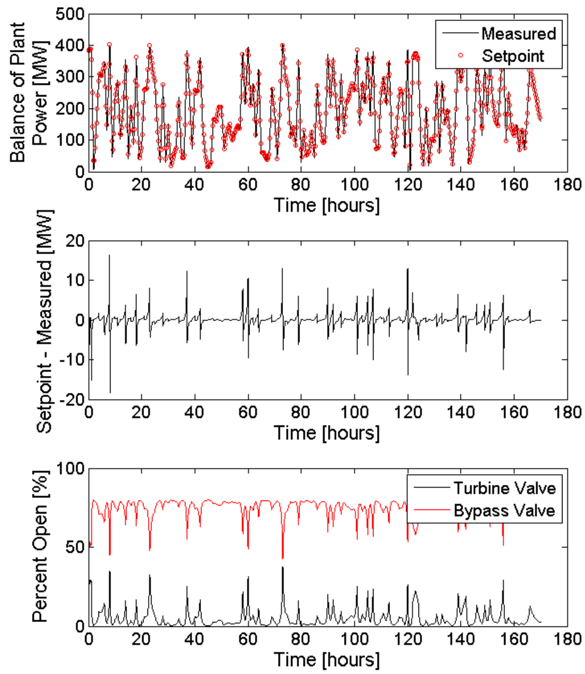

Figure 17. BOP generated power compared to the set point provided by the SC system. The dynamic behavior of the turbine and bypass valves work together to meet the specified power and dampen impacts on the connected subsystems.

Figure 18 presents the overall ability of the tightly coupled energy system to meet the electricity demand profile. The ability of the system to meet the demand is a complicated problem. An important factor in this current result is the ES, which has a limited capacity to provide for portions of time during which excess electrical energy was lost due to storage being at maximum capacity. Furthermore, the electricity could not be provided because the capacity had reached a minimal charge limit. As each subsystem physics and controller tuning is included and improved, the ability of the NHES system to meet the demand will vary.

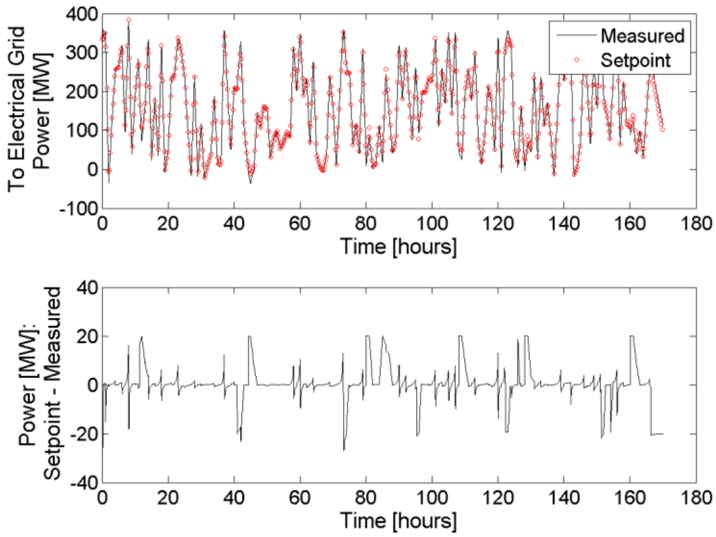

Figure 18. Result of power delivered to the grid compared to set point demanded. Periods of over- and under-production are evident. Additional studies investigating economics and impact of subsystem capacities (e.g., energy storage capacity) will be carried out in the future.

3. DEFINITION OF SUCCESSFUL EXECUTION

Successful execution, is defined herein as the ability of the model to complete a simulation session successfully and to provide consistent solutions and simulation statistics (central processing unit [CPU] time, number of time steps, number of Jacobian calculations, etc.) over a variety of forcing functions or parameters. Once the NHES simulation platform integration with RAVEN is completed, the top-level economic optimization process will sweep a number of select model parameters and simulation control options, such as total simulation time, demand profiles, and subsystem capacities. Before the integration between the NHES simulation platform and the RAVEN control driver is carried out, it is important to explore and assess the ability of the dynamic system model to successfully handle a substantial number of off-nominal simulation parameters. The following explains the approach behind determination of success criteria of the current NHES simulation toolset. The results obtained from this investigation will be important for improving the physical system and control models and will provide bounds on the permissible optimization search space to be handled by RAVEN.

3.1 COMPUTATIONAL STABILITY

Computational stability checks for potential inconsistencies in key state variables with respect to nominal design values. Computational stability should not be confused with the system stability, such as the Lyapunov stability.

Typically, these checks search for deviations of certain variables from nominal values after a seemingly steady state is reached. These variables belong to a smaller set of state variables for which no major deviations are expected. For instance, for a properly controlled system, controlled processes such as loop pressures or average or outlet temperatures should reach a reasonable equilibrium, even if not their exact nominal value for a given set of input parameters. Significant deviation from nominal values may result from control system underperformance, or even an unstable closed loop system configuration. It might also be an indication of mathematical instability that lead to nonphysical results. These instabilities typically arise from numerical inaccuracies during the computation of nonlinear iterations.

Another source of instability may arise from improper selection of time integration time step. While a reasonably small time step is generally preferred, it is most likely an intractable approach for a large-scale system, especially for long simulation times. While the platform developed for the NHES simulations uses a solver with an adaptive time step selection, for large enough time step selections, certain physical phenomena may not be resolved fast enough as the time step is progressively made smaller. This may lead to mathematical instability. In our experience, we've observed this kind of instability issues in two-phase flow calculations, particularly in the thermodynamic equation of state calculations during phase transitions. If the system is forced through a sudden change, it may end up at a non-physical state, most likely because the time step is not sufficiently small to adequately process faster modes of the system.

It may be difficult to distinguish between computational inaccuracies due to numerical issues (nonphysical results) and improper system configuration. If the parameter space is created within an arbitrary range the bounds of which were not determined based on component or subsystem performance, the simulation most likely fails because no acceptable solution can be found that satisfies the system of equations. This is a physical result. For example, the parameter space is searching within an arbitrary range for a length and/or diameter of pipe. If associated component parameters such as the pump performance curve for a loop are not properly selected to satisfy the physical requirements (e.g., loop pressure drop, or desired/required coolant velocity), it may lead to a configuration in which no physical solution can be found.

The RAVEN driver only provides the high-level subsystem sizing or capacity; the necessary translation of component sizing or performance optimization is not carried out by the model. This is a significant gap in capability. While the top-level optimization loop executed by RAVEN searches for an optimal system configuration, the subsystems may be performing at a suboptimal level, as components are not automatically reconfigured.

3.2 INTEGRATED SYSTEM

The NHES conceptual design is evolving. While certain subsystems of the integrated system model have sufficiently detailed description, such as the nuclear reactor primary heat transport subsystem or the BOP subsystem, other subsystem models, such as the IP plant or the ES battery, are relatively immature as the design information is either non-existent, or publicly unavailable.

Lack of design details may lead to unrealistic subsystem responses, such as the erroneous calculation of rate of heat transfer or pressure drop, which should affect the dynamic response of connecting subsystems.

4. METHODOLOGY FOR TESTING SUCCESSFUL EXECUTION

4.1 PARAMETER SPACE

Parameters belong to two major classes: (1) simulation control parameters, and (2) model parameters. Simulation parameters control the overall solver behavior while the model parameters change the physical systems of the model. Some generic examples of each group are shown in Table 3. These parameter classes are briefly discussed below.

Table 3. Examples of the two distinct divisions of parameters able to be set for a simulation

Type	Parameter
Simulation Parameter	Tolerance
	Increments
	Simulation time
	Solver
Model Parameter	Pipe diameters
	Pump speeds
	Nominal conditions

The successful simulation of the dynamic NHES model will be evaluated by varying a selection of parameters over a range of values. Initially, the values will be chosen based on an attempt to aggressively span the range over logical possibilities. Using a large range of simulations helps inform a follow-up study using a narrower selection of parameters, and it stresses the system to show limitations that may be unintentionally coded into the physical model so that they can be addressed.

4.1.1 Simulation Control Parameters

These parameters are outside the model design space, but they determine the execution of the simulation. They include integration algorithm, solver relative (or absolute) tolerance, and sampling frequency. The Modelica time integration solvers determine step sizes internally, which implies that sampling frequency could solely be selected based on limiting the output file size. Selection of a reasonable sampling frequency is important particularly for prolonged simulations in which the system dynamics are monitored over a period of days, weeks, or months and can lead to excessively large files. However, potential links between time solutions and the sampling frequency based on the model (e.g., external control signals sampling) must be considered to avoid erroneous results.

This category of simulation parameters includes transient forcing function parameters such as start time, duration, amplitude, and ramp rate (i.e., how quickly a variation is introduced). These investigations are not included as part of the analysis addressed in this report.

4.1.2 Model Parameters

These parameters control the physical behavior of the system. Control systems gains and time constants, nuclear reactor feedback coefficients, piping diameters and lengths, set point limit, etc., all fall into categories of model parameters. The value of model parameters should be informed by modeler experience and the physical requirements of the system. For example, excessive pipe length variations may lead to large pressure drops that may not have been properly compensated in the model. Improper model parameters can lead to simulation failure due to the inability of the solver to not find solutions at some point in the simulation or physical limits such as tank levels overflowing. Proper consideration of the physical limitations of the model parameters is important to simulation success.

4.2 EVALUATION OF RESULTS

The results of simulations run are examined using high-level results such as pass/fail, time to simulate, ability to follow demand signals, etc. As patterns or trends emerge from a higher-level examination, individual runs are then examined (e.g., error reports and impact of individual parameters) to better understand simulation results.

4.2.1 Statistical Approach

The primary method for gleaning useful information from a large number of simulations is to perform a statistical regression on the results. Since the success of a simulation is a binary outcome of success or failure, the Probability Unit (Probit) regression is used to investigate results. The independent variables are the varied simulation parameters while the outcome (success/fail) is the dependent variable. A simulation fails if Dymola indicates its failure directly (e.g., the physical limitation of the model is reached, or convergence to a solution at a given time step is not achieved), or if the total elapsed CPU time reaches a fixed limit. A time limit failure is necessary as simulations can often get stuck at some point in the simulation without an explicit failure report. For the purposes of this study, a time limit failure is classified as a failure.

To evaluate the parameters which are significant in successful model execution, the Probit regression was run using the `glmulti` automated model selection library (Calcagno 2010) available in the statistical analysis tool R (R Foundation 2017). The `glmulti` tool identifies all the possible combinations of models based on the independent variables and performs the specified regression using each of the model combinations. The quality of each of the regressed models are then evaluated using the Akaike information criterion (AIC or IC) which estimates the quality of any given model relative to all other models. The AIC is used over the p-value test as it also accounts for collinearity between the independent variables. A classification table is also used to investigate the potential for bias in the measure of the goodness of the regression. For example, if the majority of the simulations are failures the regression may indicate a good fit simply because it can predict failure every time. The classification will indicate the accuracy of the predicted vs. observed results and therefore provide additional insight.

5. RESULTS

Two sets of simulations were performed to investigate the limits of successful simulation of the NHES model. The first simulation set focused on a broader range of parameter setting values to sample the simulation space and gauge where the better areas for successful simulations lie, as well as possible issues that may arise using a one-day simulation period. The second set of simulations narrowed the number of parameters varied, refined the parameter values, and extended the simulation period to a full week. Results from each study and the information gleaned are further discussed below.

5.1 COMPUTE PLATFORM

The simulations were performed on a high-performance computational (HPC) cluster managed by the ORNL Reactor and Nuclear Systems Division (RNSD). The cluster runs on 64-bit Linux Red Hat 2.6.32 (x86_64). The cluster includes a head node and forty compute nodes. The head node has 16 2800-MHz CPUs with a total of 32-GB memory. Each compute node has 32 2400-MHz CPUs with a total of 132-GB memory.

The execution of the simulations was accomplished using the license-free binary file dymosim generated by the Dymola user interface. The executions were tested with two most recent versions, Dymola 2017 and Dymola 2017 FD01. For successful execution of the binary, either Dymola Linux version must be installed on the compute platform, or the shared libraries that come with the Dymola distribution must be made available. The list of the shared library files is extensive; they are located under the following two locations: $DYMOLA/bin/lib and $DYMOLA/bin/lib64, where $DYMOLA environment variable refers to the installation location of the software distribution. For Dymola 2017 FD01, the software is typically installed under /opt/dymola-2017FD01-x86_64/ by the standard package installer.

The compilation and binary linkage was carried out on a Parallels Ubuntu 16.04 LTS virtual machine (VM) running on a Mac OS X Yosemite 10.10.5 with 4-GHz Intel Core i7 processor with 32-GB DDR3 RAM at 1600 MHz. The Linux VM was configured to have 4 cores, 8192-GB RAM. The Ubuntu 16.04 base version comes with gcc version 5.4.0 with x86_64-pc-linux-gnu as the target. Another C compiler, clang version 3.8.0-2ubuntu4 (tag/RELEASE_380/final), was installed using the apt-get utility in order to examine potential acceleration options with alternative platforms. Testing using commercial compilers was not carried out due to unavailability. Further acceleration may be possible using more mature instrument profiling tools that come with commercial compiler packages.

Both clang and gcc compilers can generate either a 32-bit or 64-bit target binary.

5.2 DAY-LONG SIMULATION SET

The first simulation was used to gauge the overall success limits of the model under a wide range of simulation settings. The variation of settings provided the first step in identifying proper simulation settings to increase the overall likelihood of obtaining successful simulations, and it also provided significance testing of model parameters on successful simulations. Table 4 presents the settings varied for the first simulation set.

Table 4. Day-long simulation set parameter space to investigate parameter significance and simulation limits

Type	Parameter	Value
Simulation Parameter	Tolerance	1e-4, 1e-6, 1e-8, 1e-10 [-]
	Increments	10, 60, 1800, 5400 [s]
	Simulation time	1 [day]
Model Parameter	ES Capacity	4, 20, 100 [MWhr]
	Pipe length to BOP from EM	1, 1000 [m]
	Pipe length to IP from EM	1, 1000 [m]
	EM Splitter volume	10, 100 [m^3]
	EM Mixer volume	10, 100 [m^3]
	Total number of simulations:	**768**

Table 5 presents the overall results of the day-long simulation set. This high-level summary demonstrates the impact parameters can have on the successful outcome of the simulation. For example, Figure 19 demonstrates that all the simulations with a tolerance setting 1e-10 failed. The average output file size is also listed for two time increments (others scale directly proportional to the increment or the number of recorded values). File size can be a concern based on length of simulation, available storage, and data processing limitations (e.g., buffer errors). The net energy difference provides insight on how well the set point demand signals were followed, giving credit to periods of over or under production. The absolute energy difference provides an overall report on the total deviation from the set point that incurred throughout the simulation. In effect these energies inform how much energy was necessary to be provided/absorbed by the electrical grid which can be factored into an overall system performance figure of merit.

Table 5. Summary of a select number of high-level overall simulation set statistics

Parameter	Value ($\bar{x}$ +/- σ)
Success, Fail, Total	257, 511, 768
Success Rate	33 %
Output File Size: 10, 60 [s]	141, 25 [MB]
Of the Successful Runs	*($\bar{x}$ +/- σ)*
Elapsed CPU Time	3147 +/- 1339 [s]
Number of Events	76 +/- 18 [-]
BOP Net Energy Difference*	-2.1e4 +/- 1.3e4 [MJ]
BOP Abs Total Energy Difference	7.3e4 +/- 1.0e4 [MJ]
* negative energy indicates under production (i.e., setpoint – measured)	

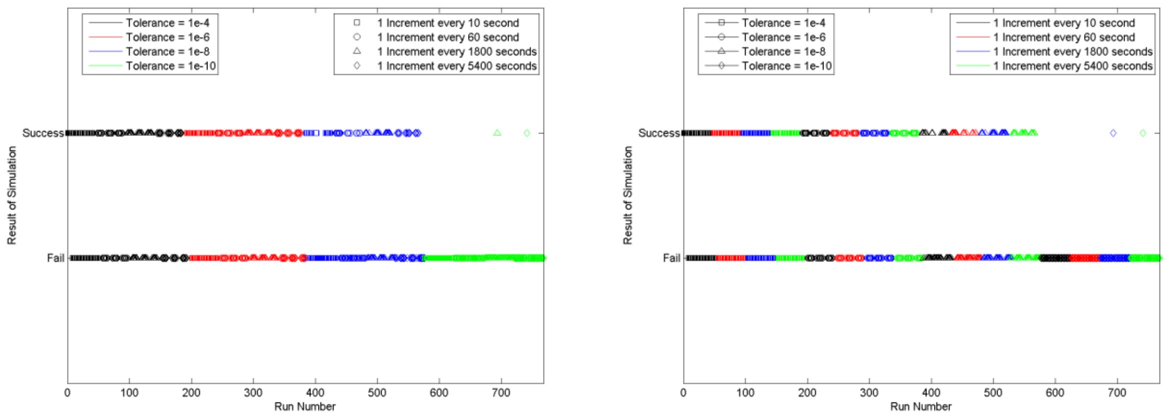

Figure 19. Two views of the same data set plotting success vs. failure simulation outcomes categorized by tolerance and increment showing the impact on the successful outcome of a simulation.

Of the simulations that ran to completion there is significant deviation between the behavior of the models as shown by the standard deviation (σ) as compared to the mean ($\bar{x}$) of the values in Table 5. Much of this deviation is likely dependent on the simulation parameter increments (Figure 20). During simulation, hourly demand data are read from an external file and linearly interpolated. If the incremental value is relatively large compared to the set point intervals, then control signals to the NHES can vary dramatically. The correct behavior of Figure 20 is the black line with the lower increment value. The behavior associated with increment value and system response attributed to following set points is important to factor into setting simulation settings.

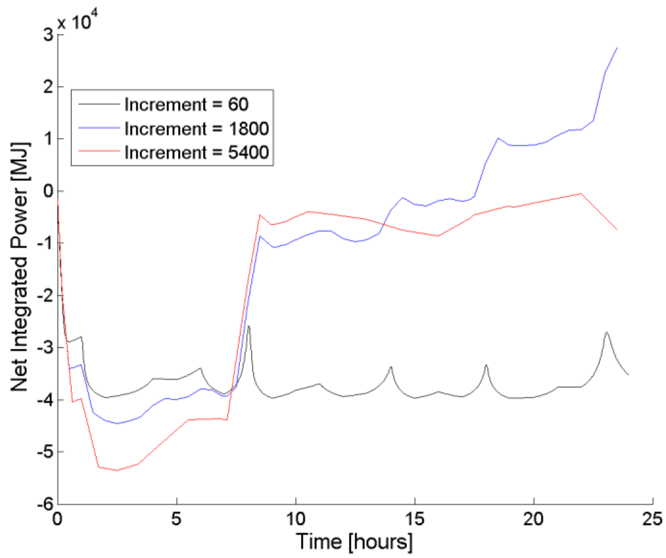

Figure 20. Demonstration of increment (in seconds) setting impact on simulation results for three successful simulations. The black curve is the correct/expected behavior, while the other two curves' sampling rates are too low, leading to erroneous results.

Using Probit regressions, the successful vs failure outcome was analyzed to determine if it was predictable and to identify which parameters were significant in determining the successful outcome. Figure 21 presents the IC profile for 100 regressed models. The red line indicates the minimum AIC value plus 2 and is often used to specify the cutoff for the "best" models. In this study, a family of potential models could be used given the natural divisions in the plot, however only 6 models were below the cutoff. Figure 22 provides a ranking of the significance of each of the independent variables in the regression models. The summary of the best regression model is shown in Table 6 which only includes the top three variables from Figure 22.

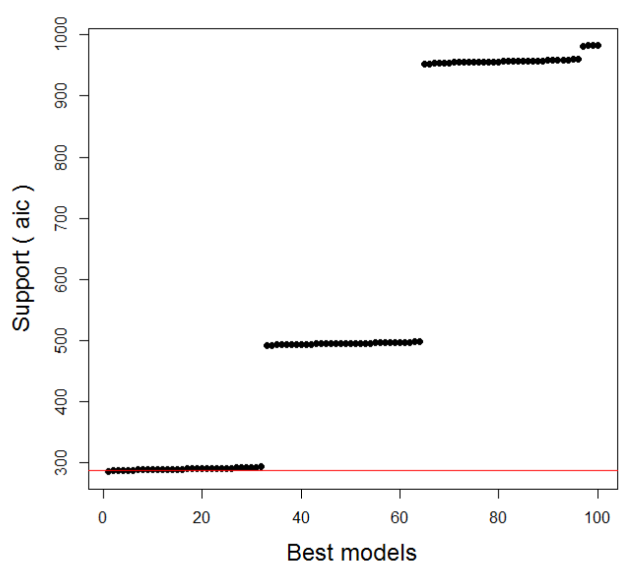

Figure 21. IC profiler of the Probit regression results for 100 variation of the regressed model. Models that lie below the red line are the models that best predict the data from the combinations examined. The natural divisions in the plot arise from the additional of an additional parameter into the regression.

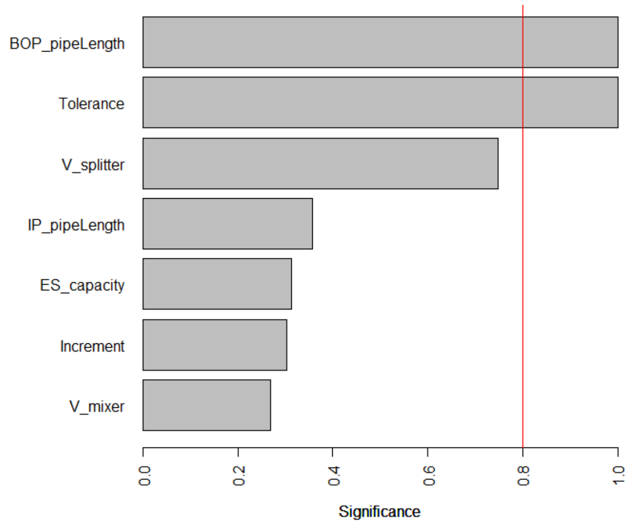

Figure 22. Plot ranking the significance of each of the independent variables on the quality of the Probit regression. The red line provides a rough cutoff of significant parameters. In this study the top three variables are all potentially significant.

Table 6. Statistical summary of the best Probit regression

Parameter	Coefficient	Std. Error	z value	Pr(>|z|)
Intercept	0.061	0.21	0.286	0.775
Tolerance	2.2e6	2.6e5	8.429	<2e-16
Pipe length to BOP from EM	-0.22	0.17	-1.356	0.1751
EM Splitter volume	-0.004	0.0019	-2.042	0.0411
AIC	**286**			

An important aspect of the analysis not yet covered is a potential bias in the predictive model due to a significant number of failed simulations (~2/3). The classification table (Table 7) demonstrates that there is no bias, therefore the regressed model accurately predicts both successful and failed simulations. This simulation set and analysis provides critical information on parameter significance which informed the subsequent week-long simulation set.

Table 7. Classification table demonstrates accuracy of regressed model in predicting successful outcomes

(S – success, F – fail, Obs – observed, Pred – predicted)

	F-Pred	S-Pred	Total
F-Obs	507	4	511
S-Obs	69	188	257
Total	576	192	768
Accuracy	0.88	0.98	0.90

5.3 WEEK-LONG SIMULATION SET

The second simulation set focused on longer term simulations which are ultimately the focus of the economic cost optimization study to be performed with RAVEN. The set of 12 – one week simulations was performed as indicated in Table 8, with a high-level summary provided in Table 9. This more concise data set of successful simulations using appropriate increment values, demonstrate limited variance between the successful runs and provides confidence that even without significant improvements to the model, the economic optimization process can likely successfully simulate over a large parameter space if the appropriate simulation parameter values are set.

Table 8. Week-long simulation set parameter space to investigate parameter significance and simulation limits

Type	Parameter	Value
Simulation Parameter	Tolerance	1e-8 [-]
	Increments	10, 30, 60 [s]
	Simulation time	7 [day]
Model Parameter	ES Capacity	20 [MWhr]
	Pipe length to BOP from EM	1, 100 [m]
	Pipe length to IP from EM	1 [m]
	EM Splitter volume	10 [m^3]
	EM Mixer volume	10, 100 [m^3]
	Total number of simulations:	**12**

Table 9. Summary of a select number of high-level overall simulation set statistics

Parameter	Value ($\bar{x}$ +/- σ)
Success, Fail, Total	12, 0, 12
Success Rate	100 %
Output File Size: 10, 60 [s]	986, 176 [MB]
Of the Successful Runs	*($\bar{x}$ +/- σ)*
Elapsed CPU Time	331 +/- 5 [min]
Number of Events	270 +/- 2 [-]
BOP Net Energy Difference	-3.7e4 +/- 1.6e2 [MJ]
BOP Abs Total Energy Difference	2.9e5 +/- 2.7e2 [MJ]

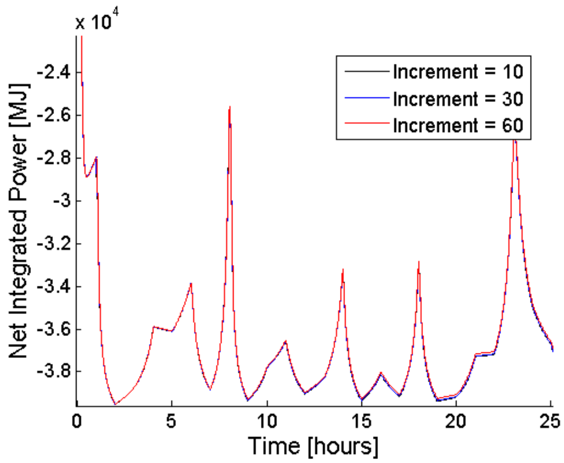

Figure 23. Demonstration of increment (in seconds) setting impact on simulation. Each of the simulations follow the appropriate trajectories as compared to large increment settings depicted in Figure 20.

Figure 24 demonstrates where the simulation spent its CPU time and when numerical events occurred over the course of the simulation for a representative simulation run. Both the values are cumulative reports. Therefore, increases in the slope indicate that more CPU time is being spent or additional events have occurred. The figure demonstrates that there are no significant changes in slope throughout the simulation. Therefore, the current NHES model appears to behave consistently throughout the simulation.

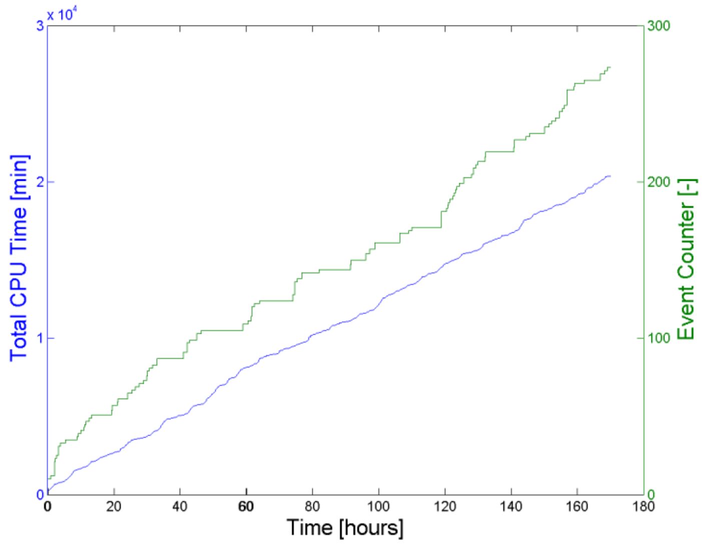

Figure 24. Plot of locations of event generation and CPU time as a function of simulation time. The lack of significant slope changes in the CPU time demonstrate that there are no particularly difficult regions of the simulation that require more processing time than others, so the model is well behaved.

5.4 ADDITIONAL SIMULATION STUDIES

Additional investigations into the various simulation and pre-simulation (i.e., executable generation flags) were made to identify areas that may improve simulation speed and overall performance. These are highest-level parameters that can be adjusted for simulation, and include the following:

- Simulation start time (set to 0)
- Simulation stop time (set to 93600 s for daily simulations and 612,000 s for weekly simulations), and
- Output interval length (set to 10)

5.4.1 Solver Parameters

These parameters select the solver algorithm and passes the required parameters to the solver. These include the following:

- Algorithm (typically set to `Esdirk45a - order 5 stiff` unless otherwise noted), and
- Tolerance (typically set to a value between `1E-09` and `1E-07`).

5.4.2 Compiler and Linker Selection and Parameters

Dymola 2017 FD01 Linux distribution was reported to be tested with two C compilers: `gcc` and `clang`. By default, Dymola invokes `gcc` as the compiler, which then invokes either `ld` or `llvm` linker depending on the system configuration.

The compilation and linking is executed by a shell script stored under `$DYMOLA/insert/dsbuild.sh`. The default invocation line for the `gcc` compiler is the following:

```
$CC -o dymosim $DEF $INC $SRCS $LIB
```

where the C compiler, `CC`, is defined as follows:

```
CC="cc -O0 -Wl,--no-as-needed"
```

The C compiler, `cc`, by default invokes `gcc`.

The important flag for the compiler command is `–O`, which determines the level of optimization tasks to be carried by the linker. For The `–O` flag takes the following arguments:

- `-O<number>` set optimization level to `<number>`,
- `-Os` optimize for space rather than speed,
- `-Ofast` optimize for speed disregarding exact standards compliance, and
- `-Og` optimize for debugging experience rather than speed or size.

This flag is by default set to `-O0`, which performs no optimization for the generated binary, for safe execution, and to avoid potential conflicts between libraries.

In order to benefit from binary generation optimization, the –O flag was tested with various optimization levels, i.e., `-O1`, `-O2`, `-O3` and `-Ofast`. It was determined that the `-O3` option provides about 40% speedup compared to a non-optimized binary. To achieve that, the compiler definition variable in the `dsbuild.sh` script file was changed as follows:

```
CC="cc -O3 -Wl,--no-as-needed"
```

The effect of speedup is demonstrated in Figure 25 where some of the simulation options and parameters are provided in the legend. Figure 25 shows only part of the simulations, which were executed until 93600 sec. Either gcc or clang was used as the compiler, and different levels of optimization were tested. Also tested was solvers with different relative error tolerances. While Dymola comes with many more built-in solvers, only `ESDIRK45a` and `CVODE` integrators were able to successfully initialize and run the simulations. As a stiff solver, `ESDIRK45a`, successfully worked in a wide variety of tolerances while `CVODE` only worked with a tighter error tolerance.

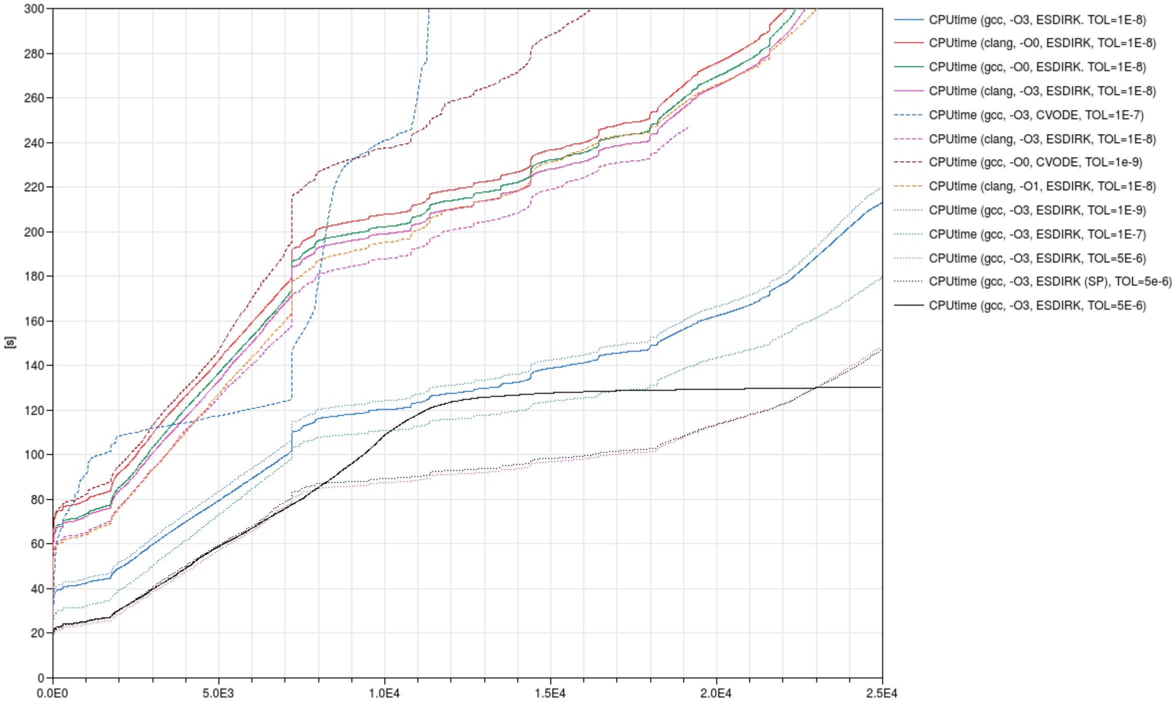

Figure 25. Comparison of various execution options.

Dymola 2017 FD01 comes with a support for sparse solvers (available only with the `CVODE`solver) using a multithreaded (OpenMP) variant of SuperLU algorithm. If a model is sparse and sufficiently large, Dymola automatically generates a warning to test the sparse solvers. This option can be enabled using the following command:

```
Advanced.SparseActivate=true
```

It may be possible to gain some speedup with this option; however, as the `CVODE` solver did not successfully work for a variety of simulation parameters, it was not used in the bulk tests documented in this report.

Finally, starting from a proper initial state helps gain significant speed-up for the daily simulation. The data traces in Figure 25 (for the entire simulation) typically finish up in approximately 1000 sec. for the non-optimized simulations, and around 600 sec. for optimized simulation (using `gcc -O3`), all simulated to 93600 sec. (a little over a day), which delivers a performance improvement around 40%.

Using the steady state initialization, the simulation performance can be greatly improved. For instance, initializing from a steady state, and taking advantage of the gcc -O3 optimization process, the total simulation time, i.e., simulation duration of 93600 sec., can be dropped below 300 sec., which is a speed-up of about 2, from the optimized solution, and a speed-up of over 3 from the non-optimized solution.

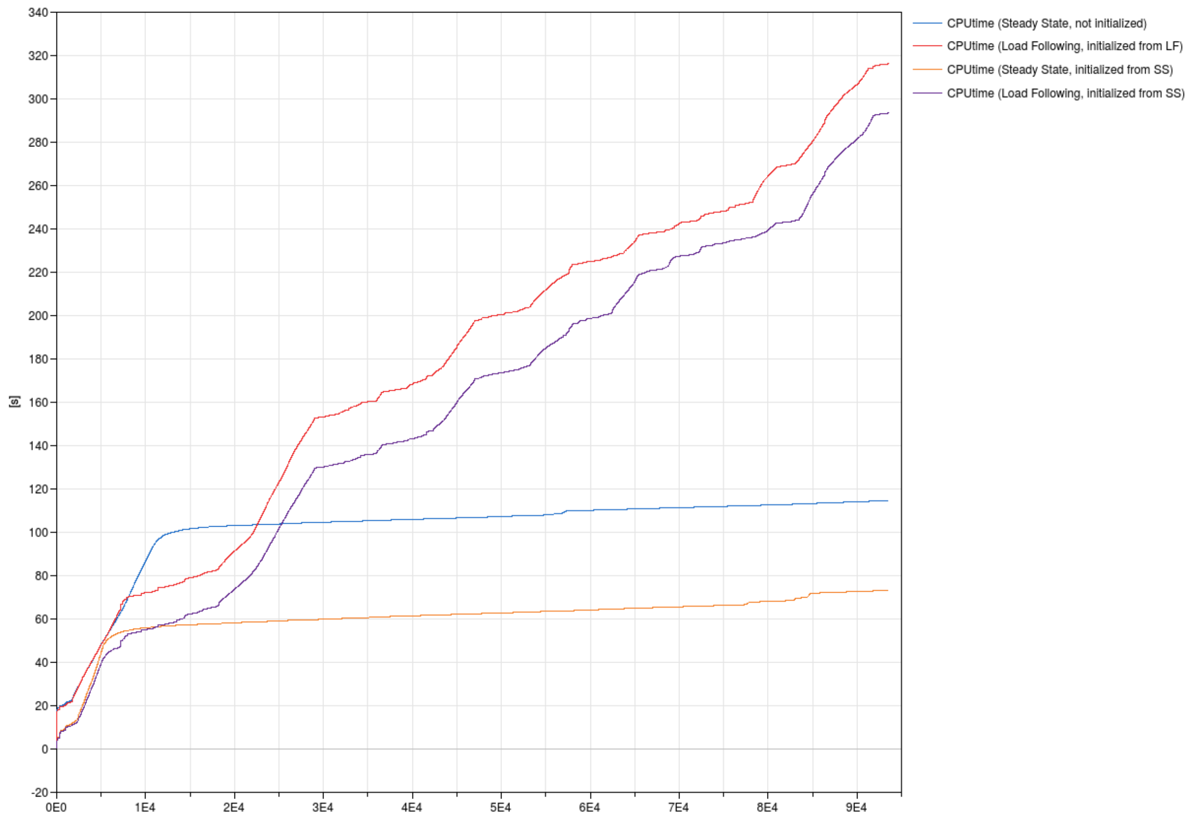

Figure 26. Further acceleration of simulation performance using steady state initialization.

6. CONCLUSIONS AND FUTURE WORK

6.1 CONCLUSIONS AND RECOMMENDATIONS

A procedure for investigating the potential simulation space of the NHES model has been developed to provide guidance of parameters which will increase the likelihood of simulation success and to help identify potential issues in the physical model’s implementation that should be addressed. This procedure analyzed the parameter space of the current implementation of a nuclear reactor coupled with a high-temperature electrolysis plant. The most important parameter for obtaining a successful outcome was found to be the tolerance parameter in the time integration solver followed by the increment time parameter. It is recommended that tolerance settings within the range of 1e-4 and 1e-8 and increment settings between 10-60 seconds be employed to provide the greatest likelihood of success (using the Runga-Kutta: esdirk45a solver). Model parameters have a much more diminished impact on a successful outcome than the simulation parameters. However, model parameters outside a reasonable range (e.g., excessive pipe lengths) will decrease the likelihood of success, so engineering judgment will be required to define what is reasonable. Model improvements will also be made (e.g., industrial process, pressurizer, mixer volume) to improve the simulation success rate and overall performance. The prescribed procedure will continue to be used in future revisions of this and other NHES models to improve system model performance and to provide guidance for additional tools such as RAVEN.

We recommend that available compiler technologies be tested, and the results validated. If commercial compiler packages are available, their advanced optimization tools may provide great benefit in terms of resource utilization and performance improvement.

6.2 FUTURE WORK

The results presented in this report are generated from an NHES integrated system model that employed idealized components for successful execution and performance gain. Maturation of individual components and overall sub-systems will be considered in future work. Improving the realism of the physical models will provide critical information on the limitation of dynamic operations of the NHES and provide key information for subsequent economic and reliability analysis. Examples include the condenser, condensate booster pumps in the balance of plant subsystem, and the compressor in the gas turbine subsystem. Additionally, options to improve simulation efficiency will continue to be investigated by examining available handles such as optimization flags and potential for parallelization. Improvements to physical models and control systems will also be made to reduce the number of events generated during the solution process. Each of these areas will provide important improvements for ultimate integration into the economic optimization analysis to be performed with RAVEN.

7. REFERENCES

Bragg-Sitton, S. M., Boardman, R., Ruth, M., Zinaman, O. 2015. "Rethinking the Future Grid: Integrated Nuclear Renewable Energy Systems." Report no. NREL/CP-6A20-63207.

Calcagno, V., Mazancourt, C. 2010. "glmulti: An R Package for Easy Automated Model Selction with (Generalized) Linear Models." *Journal of Statistical Software*. Vol. 34, Iss. 12, May.

EIA. 2016a. "Regional Wholesale Markets: June 2016." US Energy Information Administration. https://www.eia.gov/electricity/monthly/update/wholesale_markets.cfm, August.

—. 2016b. "Wholesale Power Prices Decrease Across the Country in 2015." US Energy Information Administartion. http://www.eia.gov/todayinenergy/detail.cfm?id=24492, August.

EPRI. 2015. "Program on Technology Innovation: Fossil Fleet Transition with Fuel Changes and Large Scale Variable Renewable Integration." Electric Power Research Institute. Report no. 3002006517.

Mod. Assoc. 2017. "Modelica - A Unified Object-Oriented Language for Systems Modeling." The Modelica Association. https://www.modelica.org.

R Foundation. 2017. R Foundation for Statistical Computing, www.r-project.org, March.

Shropshire, D., Williams, K., Boore, W., Smith, J., Dixon, B., Dunzik-Gougar, M., Adams, R., Gombert, D., Schneider, E. 2007. "Advanced Fuel Cycle Cost Basis." Idaho National Laboratory. INL/EXT-07-12107.

Westinghouse. 2007. "Computer Models for IRIS Control System Transient Analysis." Report no. STD-AR-06-04.

Zaiontz, C. 2017. "Real Statistics Using Excel." http://www.real-statistics.com/, March.